In vivo imaging of Tau pathology using Multi-Parametric Quantitative MRI

Jack A Wells[1], James M O'Callaghan[1], Holly E Holmes[1], Nicholas M Powell[1], Bernard Siow[1], F Torrealdea[2], Marilena Rega[2], Ozama Ismail[1], Simon Walker-Samuel[1], Xavier Golay[2], Simon Richardson[1], Adam J Schwarz[3], Michael J O'Neil[4], Emily C Collins[3], Niall Colgan[1], and Mark F Lythgoe[1]

[1]*Centre for Advanced Biomedical Imaging, UCL, London, London, United Kingdom,* [2]*Institute of Neurology, UCL, London, United Kingdom,* [3]*Lilly Corporate Centre, Eli Lilly & Co. Ltd, Indianapolis, United States,* [4]*Eli Lilly & Co. Ltd Erl Wood Manor, Windlesham, Surrey, United Kingdom*

Introduction A key neuropathological hallmark of Alzheimers Disease(AD) is the presence of intracellular neurofibrillary tangles(NFTs) of hyperphosphorylated Tau protein[1]. There is a need for greater understanding of the relationship between tau burden and non-invasive imaging data for improved diagnosis and therapeutic assessment of this devastating disease[2]. In this work, a mouse model of tauopathy was used to investigate how elevated tau expression affects the clinically implementable MRI parameters: i) cerebral blood flow (CBF) using arterial spin labelling (ASL) ii) amide proton transfer(APT) using chemical exchange saturation transfer (CEST) iii) brain glucose metabolism using glucoCEST iv) the diffusion properties of tissue water using diffusion tensor imaging (DTI) v) brain morphology using high resolution 3D structural imaging with tensor based morphometry (TBM). This is the first application of ASL, CEST and DTI to the Tg4510 model as well as glucoCEST to investigate neurodegenerative disease.

Methods 9 transgenic Tg4510 and 17 wild-type(WT) litter matched mice(8.5month) were imaged using a 9.4T Agilent scanner for the ASL, DTI, structural, and CEST data. The glucoCEST data was acquired using a second cohort of 5 transgenic Tg4510 and 5 WT litter matched(9.5 month) mice. RF transmission was performed with a 72 mm inner diameter volume coil and a 4-channel receiver coil (Rapid Biomedical). Mice were then anesthetized using 2% isoflurane and 1 L/m O_2 which was reduced 1.5% and 0.5 L/m O_2 during imaging using the following parameters.

ASL : A flow-sensitive alternating inversion recovery(FAIR) sequence with a 4-shot segmented spin-echo EPI readout was implemented with parameters: 5 slices, slice thickness=1mm, FOV=20x20mm, slice selective inversion pulse width=12mm,5 inversion times.

DTI :Diffusion-weighted images and a single B0 image were acquired using a 4-shot spin echo EPI sequence. Diffusion gradients were applied in 30 directions with parameters: G=0.25T/m, Δ=9.3ms, δ=5.5ms, and b=1050s/mm2,TR=2000ms.

3D Structural Imaging: A 3D T2-weighted sequence was employed for structural imaging with parameters: FOV=19.2mm x16.8mm x12.0mm; resolution=150μm^3; TR=2500ms, TE_{eff}=43ms, ETL=4; manual segmentation of brain volumes was performed in addition to tensor-based morphometry(TBM) analysis using a fully automatic pipeline[3].

CEST: Gradient echo images (TR=6.1ms, TE=2ms, flip=5°, FOV=20×20mm^2, slice thickness 3mm, matrix size=64×64, line width <30 Hz) were acquired following a train of saturation pulses at 79 frequency offsets covering ±6 ppm to encompass APT saturation peaks around +3.5ppm. An estimate of APT was calculated as the area under the MTR_{asym} curves between 3.3 and 3.7ppm by subtracting the signal intensities at either side of the direct water saturation peak.

GlucoCEST: The animals were fasted for 24 hours prior to scanning. A 0.2 ml bolus of D-glucose with a concentration of 1g/Kg primed intraperitoneal (IP) line was inserted before positioning of the animal for imaging. CEST measurements (using identical parameters described above), were applied at baseline and then every 8 minutes following an IP injection for a total of 100 minutes following glucose delivery. To measure the in-vivo glucose uptake the chemical exchange contaminating effects are removed by subtracting pre-injection from post-injection and measuring all of the area under the glucose enhanced MTRasym curve[4]

Results All of the MRI techniques were able to discriminate between the Tau pathology and control groups mean region of interest values segmented across multiple slices(Figure 1). The Tg4510 mice had increased radial diffusivity in the corpus callosum(Fig.1a), increased CBF in the frontal cortex(Fig.1b), decreased APT in the hippocampus(Fig.1c) and increased glucoCEST signal in the motor cortex(Fig.1d). We observed a decreased hippocampal volume(manual segmentation) in the TG4510 mice(Fig.1e) which was also indicated by the TBM analysis(Fig.1f) as a reduction in grey matter in this region(red) and an enlargement in the adjacent ventricles(blue). Significant differences between the groups were also observed for some of the parameters in other brain regions not presented here.

Figure 1: Quantitative MRI measurements that discriminate tau pathology from healthy control subjects

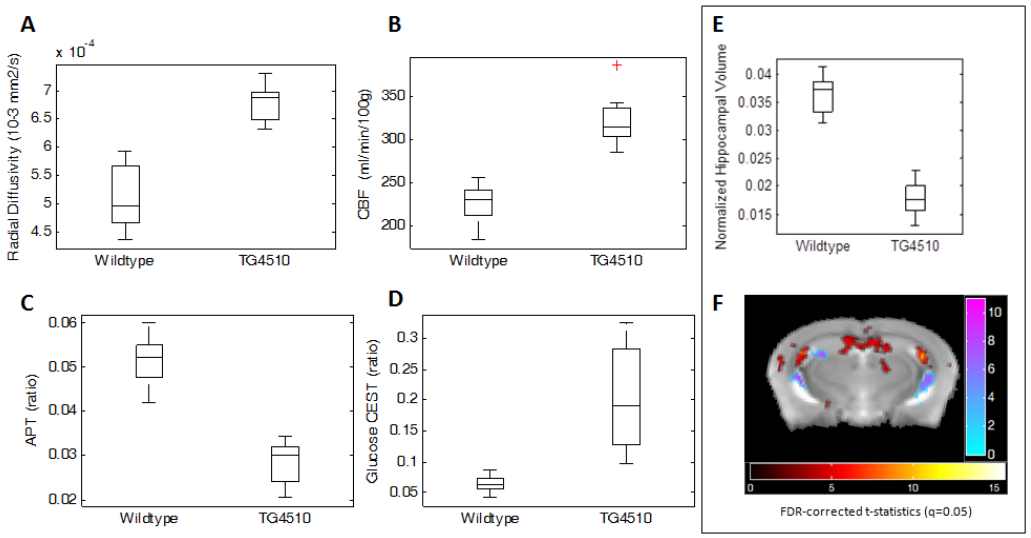

(A)Radial diffusivity in the corpus callosum, (B) CBF in the frontal cortex, (C) APT ratio in the hippocampus, (D) Glucose CEST in the cortex and (E)Volume and TBM(F) analysis in hippocampus.
A-C: n=17 WT, n=9 TG4510 (age 8.5 months). D: n=5 WT, n=5 TG4510 (age 9.5 months). E,F:16 WT, n=9 TG4510 (age 8.5 months).

Discussion This is the first study to demonstrate the sensitivity of ASL, DTI, CEST, glucoCEST and TBM to *in vivo* tau pathology in the Tg4510 mouse. These clinically relevant techniques provide a unique insight into the pathological processes associated with AD. Multi-parametric imaging biomarkers may lead to more accurate staging of the neurodegenerative cascade, and guide assessment of novel therapeutic methods. Histological staining shows that the tau pathology was well developed in the regions presented at this late imaging time point. Further work will evaluate the sensitivity of these methods to lower levels of pathology and investigate the possibility of their combination to provide an enhanced detection methodology using a multi-parametric approach.

References 1.Braak,H;J Neuropath Exp Neur;960-969;2011. 2.Langbaum, J. B,et al. Nat Rev Neurol:2013. 3.Powell,N, BCISMRM PostgraduateSymposiumProceedings:2013. 4.Walker-Samuel, S.,et al, Nature Med. 2013.